Optimization Method for Electrical Water Heaters Considering Shifting Potentials of Electricity Consumption and Water-use Activities

Yuqing Bao, *Member*, *IEEE*, Zhonghui Zuo, and Xuehua Wu

***Abstract*—Electrical water heaters (EWHs) are important candidates to provide demand-response services. The traditional optimization method for EWHs focuses on the optimization of the electricity consumption, without considering the shifting potential of the water-use activities. This paper proposes an optimization method for EWHs considering the shifting potentials of both the electricity consumption and water-use activities. Considering that the water-use activities could be monolithically shifted, the shifting model of the water-use activities was developed. In addition to the thermodynamic model of the EWH, the optimal scheduling model of the EWH was developed and solved using mixed-integer linear programming. Case studies were performed on a single EWH and aggregate EWHs, demonstrating that the proposed method can shift the water-use activities and therefore increase the load-shifting potential of the EWHs.**

***Index Terms*—Electrical water heater (EWH), demand response, load-shifting, water-use activity.**

I. Introduction

DEMAND response (DR) has been demonstrated to have a significant effect on the active balance of a power system. By taking advantage of time-varying price signals or incentive policies, electricity users can adjust their electrical power according to the requirements of power system, realizing peak-load shaving, load-shifting, or accommodating the fluctuations of renewable energies.

The development of smart metering technologies has enabled domestic appliances to participate in DR. Among all domestic DR appliances, thermostatically controlled loads (TCLs) have the greatest potential owing to their heat/cold storage characteristics. TCLs mainly include air conditioners (ACs) [1], [2], refrigerators [3], [4], and electrical water heaters (EWHs) [5], [6]. Compared with ACs and refrigerators, EWHs have the following advantages.

1) Less discomfort: unlike ACs or refrigerators, the temperature of EWHs does not need to be maintained at a comfortable level at all time. Temporarily interrupting electrical power causes less discomfort to the users.

2) Easily shifted: as the scheduling of EWHs only needs to guarantee the water temperature during water use, the allowable temperature range is wide during periods without use of water. Therefore, the load of EWHs can be shifted more easily.

Several studies have focused on DR strategies. The control strategies for EWHs can be categorized into three types: rule-based methods [7] - [9], learning-based methods [10] - [13], and model-based optimization methods [14]-[19]. Rule-based methods are realized using a group of control logic methods based on expert knowledge. The feedback control signal, e. g., EWH states [7], the required balancing reserve [8], and system frequency [9], is also required to calculate the specific control signal for EWHs to realize load-shifting or frequency control. In contrast to rule-based methods, learning-based methods consider the dynamics of the EWH system as a black box, without the need to model the entire system mathematically. Learning-based algorithms such as Q-learning [10], double Q-learning [11], fitted Q-iteration [12], and deep reinforcement learning [13], have been adopted to train the control policy of EWHs. Although effective in addressing nonconvex and nonlinear problems, learning-based methods are based on trial and error, which cannot guarantee a global optimum. Based on the mathematical models of EWHs, model-based optimization methods can determine the global optimal solution for EWHs. To implement optimization, the cost function and a group of operation constraints should be defined and then linearized or relaxed so that the problem can be solved using model-based optimization techniques such as dynamic programming [14], mixed-integer linear programming (MILP) [15]-[18], and convex programming [19].

Notwithstanding the variety of algorithms proposed for EWHs, the DR method is a key factor affecting the performance of EWHs. Among existing studies, electricity management is the most popular method for realizing DR using EWHs. Electricity management, which optimizes the heating power of EWHs, does not adjust the water-use activities. To

Manuscript received: March 24, 2023; revised: June 21, 2023; accepted: August 17, 2023. Date of CrossCheck: August 17, 2023. Date of online publication: September 19, 2023.

This work was supported in part by the National Natural Science Foundation of China (No. 51707099).

This article is distributed under the terms of the Creative Commons Attribution 4.0 International License (http://creativecommons.org/licenses/by/4.0/).

Y. Bao (corresponding author) and Z. Zuo are with School of Electrical and Automation Engineering, Nanjing Normal University, Nanjing 210046, China (e-mail: baoyuqing@njnu.edu.cn; 779520778@qq.com).

X. Wu is with School of Electrical Engineering, Nanjing Vocational University of Industry Technology, Nanjing 210023, China (e-mail: wuxuehua@niit.edu.cn).

DOI: 10.35833/MPCE.2023.000183

ensure a comfort level, the electricity management method defines the comfort level (tank water temperature) within a rigid range [7]-[12], [14], [15]. In addition to electricity management, water-use curtailing is another method for realizing DR using EWHs. Water-use curtailing is realized by allowing the tank water temperature to be below the minimum limits so that the user's comfort is sacrificed. Under these conditions, users can only use less hot water or use hot water at a lower temperature. To reflect the impact of DR on the discomfort of users, optimization usually includes the discomfort term in the objective function [13], [16]-[19].

The third DR method realized by EWHs is the shifting of water-use activities, which advances or postpones water-use activities without affecting the total water consumption. Compared with water-use curtailing, it is more realistic and acceptable for EWH users to shift water-use activities, as most users prefer postponing their bath time to having a bath at a lower temperature. However, little attention has been paid to shifting of water-use activities by EWHs.

To fill this gap, this paper proposes an optimization method that considers the water-use shifting potential of EWHs. By developing a shifting model of the water-use activities, not only the water-use activities but also the electricity consumption is optimized. A summary of different DR methods realized by EWHs is presented in Table I. A schematic of the three different ways of DR realized by EWHs is shown in Fig. 1.

TABLE I
SUMMARY OF DIFFERENT DR METHODS REALIZED BY EWHS

Way of DR			DR method	Reference
Electricity management	Shifting of water-use activities	Water-use curtailing		
√	×	×	Rule-based method	[7]-[9]
√	×	×	Learning-based method	[10]-[12]
√	×	√	Learning-based method	[13]
√	×	×	Model-based optimization method	[14], [15]
√	×	√	Model-based optimization method	[16]-[19]
√	√	×	MILP	Proposed method

The contributions of this paper are summarized as follows.

1) The load-shifting potential of EWHs was increased by considering the shifting of water-use activities, which is practical under real conditions. A corresponding optimization model was established considering both electricity management (shifting electricity consumption) and the shifting of water-use activities.

2) The nonlinear load-shifting model of EWHs was converted into a linearized form using a matrix encoding method. Based on this, the optimization model could be solved using MILP to obtain a global optimum.

The remainder of this paper is summarized as follow. In Section II, the thermodynamic model of EWHs is derived. In Section III, a shifting model of water-use activities is established. The development of EWH optimization model is described in Section IV. Testing examples are provided in Section V. Finally, conclusions are summarized in Section VI.

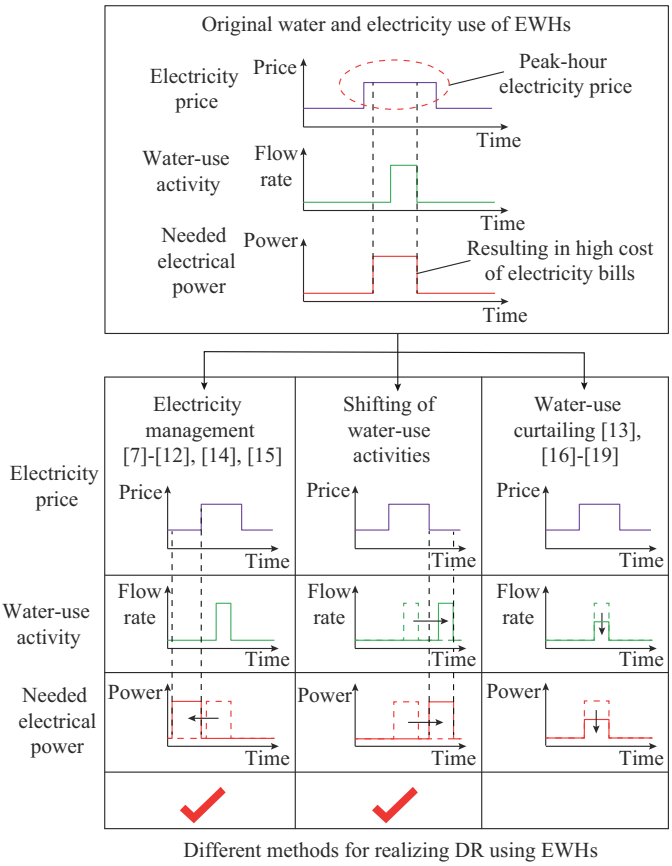

Fig. 1. Three different ways of DR realized by EWHs ("√" indicates ways adopted by proposed method).

II. THERMODYNAMIC MODEL OF EWHS

A. Thermodynamic Modeling

The schematic diagram of an EWH is shown in Fig. 2. The EWH system consists of a water tank, mixing valve, and tap. The water in the water tank is heated using electric power. When the tap is opened, hot water from the water tank is mixed with cold water to maintain the desired temperature.

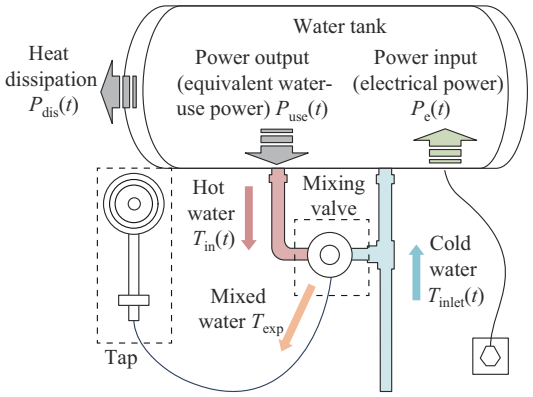

Fig. 2. Schematic diagram of an EWH.

According to the first law of thermodynamics, the change in the internal energy within the tank equals the heat added to the tank. The differential equation is formulated as :

$$\frac{\mathrm{d}E_{\mathrm{in}}(t)}{\mathrm{d}t}=P_{\mathrm{e}}(t)-P_{\mathrm{dis}}(t)-P_{\mathrm{use}}(t) \tag{1}$$

where $E_{\mathrm{in}}(t)$ is the internal energy of the water in the tank; $P_{\mathrm{e}}(t)$ is the electrical power input; $P_{\mathrm{dis}}(t)$ is the power dissipated from the tank into the environment; and $P_{\mathrm{use}}(t)$ is the equivalent water-use power.

The internal energy $E_{\mathrm{in}}(t)$ is related to the water temperature $T_{\mathrm{in}}(t)$ and can be formulated as:

$$E_{\mathrm{in}}(t)=c\rho V_{\mathrm{tank}}T_{\mathrm{in}}(t) \tag{2}$$

where c is the specific heat capacity of water; ρ is the density of water; and V_{tank} is the volume of the water tank.

The dissipation power $P_{\mathrm{dis}}(t)$, which is determined by the temperature difference between the tank and the environment, can be formulated as:

$$P_{\mathrm{dis}}(t)=\frac{T_{\mathrm{in}}(t)-T_{\mathrm{amb}}(t)}{R} \tag{3}$$

where $T_{\mathrm{amb}}(t)$ is the ambient temperature outside the tank; and R is the thermal resistance of the tank.

The equivalent water-use power $P_{\mathrm{use}}(t)$ represents the power loss caused by water use, i. e., by letting out hot water from and letting in cold water into the tank. $P_{\mathrm{use}}(t)$ can be expressed as:

$$P_{\mathrm{use}}(t)=c\rho B(t)(T_{\mathrm{in}}(t)-T_{\mathrm{inlet}}(t)) \tag{4}$$

where $B(t)$ is the flow rate of the hot water leaving the tank; and $T_{\mathrm{inlet}}(t)$ is the temperature of the cold water flowing into the tank. Note that $B(t)$ is not a fixed value, but is adjusted by the mixing valve according to $T_{\mathrm{in}}(t)$ and $T_{\mathrm{inlet}}(t)$ to maintain the tap water temperature at the desired level T_{exp}. The control algorithm for the mixing valve is defined as:

$$B(t)=B_{\mathrm{tap}}(t)\frac{T_{\mathrm{exp}}-T_{\mathrm{inlet}}(t)}{T_{\mathrm{in}}(t)-T_{\mathrm{inlet}}(t)} \tag{5}$$

where $B_{\mathrm{tap}}(t)$ is the flow rate of the tap. By substituting (5) in (4), $P_{\mathrm{use}}(t)$ can be converted into:

$$P_{\mathrm{use}}(t)=c\rho B_{\mathrm{tap}}(t)(T_{\mathrm{exp}}-T_{\mathrm{inlet}}(t)) \tag{6}$$

Substituting (2), (3), and (6) into (1) yields:

$$\frac{\mathrm{d}T_{\mathrm{in}}(t)}{\mathrm{d}t}=\frac{P_{\mathrm{e}}(t)R-P_{\mathrm{use}}(t)R-T_{\mathrm{in}}(t)+T_{\mathrm{amb}}(t)}{CR} \tag{7}$$

where C is the equivalent heat capacity of the water tank, which is defined as:

$$C=c\rho V_{\mathrm{tank}} \tag{8}$$

By solving the differential equation of (7), the discrete form of the thermal dynamics model is obtained by solving the differential equation in (7).

$$T_{\mathrm{in}}(t+1)=T_{\mathrm{in}}(t)\mathrm{e}^{-\frac{\Delta t}{CR}}+(P_{\mathrm{e}}(t)R-P_{\mathrm{use}}(t)R+T_{\mathrm{amb}}(t))\left(1-\mathrm{e}^{-\frac{\Delta t}{CR}}\right) \tag{9}$$

where Δt is the step size of the scheduling horizon.

B. Overall Structure of Price-based DR Realized by EWHs

Figure 3(a) presents the overall structure of EWHs participating in price-based DR. The participation of EWHs in price-based DR can be divided into three layers: the power system operator (PSO) layer, load aggregator (LA) layer, and electricity user layer. The interaction between the LAs and the PSO is established through bidding or long-term contracts to realize the supply-demand interaction of the aggregate users' power. Price-based DR is implemented between the LAs and users or directly between the PSO and users. When participating in the DR, users receive price signals sent by either the LAs or the PSO while considering electricity-consumption shifting and water-use shifting for optimization. After the optimized results are obtained, the control signals are sent to the EWHs to obtain the actual electrical power $P_{\mathrm{e}}(t)$.

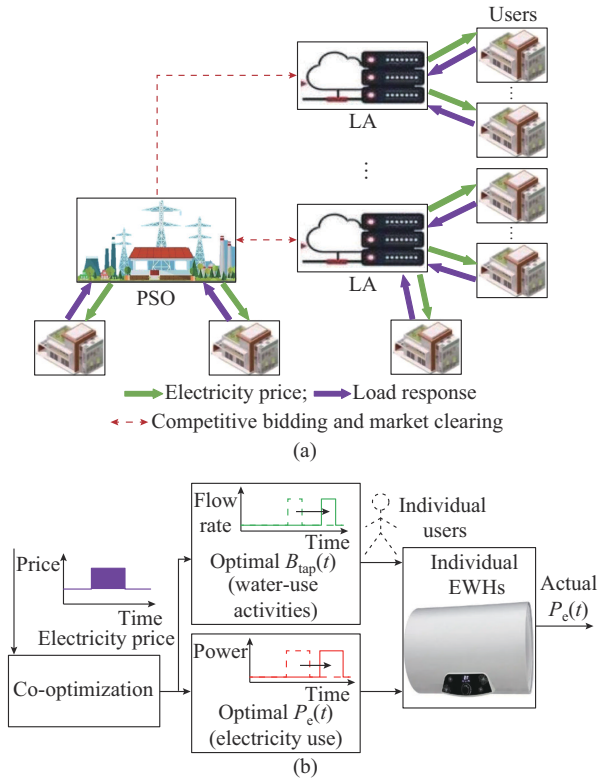

Fig. 3. Schematic of price-based DR using EWHs. (a) Overall structure of EWHs participating in price-based DR. (b) Price-based DR of individual users.

The electricity consumption and water-use activity to be optimized are represented by $B_{\mathrm{tap}}(t)$ in (6) and $P_{\mathrm{e}}(t)$ in (9), as shown in Fig. 3(b).

III. Shifting Model of Water-use Activity

The load-shifting of the water-use activity results in water use ahead of or after the original schedule. The water-use activity is represented by the tap flow rate $B_{\mathrm{tap}}(t)$, and the original curve of the flow rate (before shifting) can be defined as $\boldsymbol{B}_{\mathrm{tap0}}=[0,\ldots,B_{\mathrm{tap1}},B_{\mathrm{tap2}},\ldots,B_{\mathrm{tap}d},\ldots,0]$, where B_{tap1}, B_{tap2}, …, $B_{\mathrm{tap}d}$ are the nonzero elements of $\boldsymbol{B}_{\mathrm{tap0}}$, and d is the number of nonzero elements in $\boldsymbol{B}_{\mathrm{tap0}}$. Assuming $\boldsymbol{B}_{\mathrm{tap0}}$ can be monolithically shifted in the scheduling horizon, the solution space of $B_{\mathrm{tap}}(t)$ can be represented as:

$$\boldsymbol{B}_{\text{tap},s}=\begin{bmatrix} B_{\text{tap1}} & B_{\text{tap2}} & \cdots & 0 \\ 0 & B_{\text{tap1}} & \cdots & 0 \\ \vdots & \vdots & & \vdots \\ B_{\text{tap2}} & B_{\text{tap3}} & \cdots & B_{\text{tap1}} \end{bmatrix} \tag{10}$$

$\boldsymbol{B}_{\text{tap},s}$ contains every possible curve of $B_{\text{tap}}(t)$, and every row in (10) represents a potential profile of $B_{\text{tap}}(t)$, which can be described by the vector $\boldsymbol{B}_{\text{tap}}=[B_{\text{tap}}(1), B_{\text{tap}}(2), \ldots, B_{\text{tap}}(N_{\text{t}})]$. By introducing a 0-1 binary variable $y(t)$ that indicates the row number of $\boldsymbol{B}_{\text{tap}}$ in $\boldsymbol{B}_{\text{tap},s}$, $\boldsymbol{B}_{\text{tap}}$ can be calculated as:

$$\boldsymbol{B}_{\text{tap}}=\begin{bmatrix} y(1) & y(2) & \cdots & y(N_{\text{t}}) \end{bmatrix}\boldsymbol{B}_{\text{tap},s} \tag{11}$$

where N_{t} denotes the number of time steps in the scheduling horizon. Note from (10) and (11) that the value of $y(t)$ also represents the start time of the water-use activity. $y(t)=1$ indicates that water use starts at time t. Variable $y(t)$ should satisfy the uniqueness constraint:

$$\sum_{t=1}^{N_{\text{t}}} y(t)=1 \tag{12}$$

To calculate the specific starting time of a water-use event, an auxiliary 0-1 binary variable $z(t)$ is introduced to construct the following constraint:

$$z(t)-z(t+1)=y(t) \tag{13}$$

Equation (13) provides every $z(t)=1$ before water-use activity and every $z(t)=0$ after water-use activity. Using $z(t)$, the starting time of water-use activity t_{s} can be obtained as:

$$t_{\text{s}}=\sum_{t=1}^{N_{\text{t}}} z(t)\Delta t \tag{14}$$

To guarantee the tap temperature T_{exp} during water use, the mixing valve requires the tank water temperature $T_{\text{in}}(t)$ to be higher than T_{exp} during water use, as shown in Fig. 4.

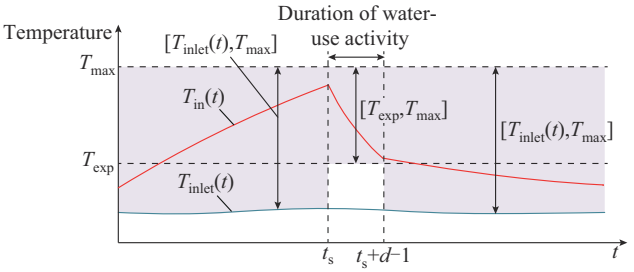

Fig. 4. Allowable range of tank water temperature $T_{\text{in}}(t)$.

The water temperature constraint can be formulated as:

$$\begin{cases} T_{\text{exp}} \le T_{\text{in}}(t) \le T_{\max} & t_{\text{s}} \le t \le t_{\text{s}}+d-1 \\ T_{\text{inlet}}(t) \le T_{\text{in}}(t) \le T_{\max} & \text{else} \end{cases} \tag{15}$$

where $T_{\max}$ is the maximum water temperature limit of the tank. The first condition in constraint (15) cannot be directly solved using MILP. To address this problem, the originally defined $y_{\text{tap}}(t)$ and newly defined binary variable $u(t)$ are introduced to convert (15) into the following equivalent form:

$$\sum_{i=0}^{d-1} y(t+i)=u(t+d-1) \tag{16}$$

$$T_{\text{inlet}}(t)+u(t)(T_{\text{exp}}-T_{\text{inlet}}(t)) \le T_{\text{in}}(t) \le T_{\max} \tag{17}$$

It can be observed from (16) and (17) that $u(t)$ represents whether time t is during the water-use activity. $u(t)=1$ indicates that water is used (the tap outputs water) at time t.

A schematic of the shifting model is provided in Fig. 5, which shows examples of $\boldsymbol{B}_{\text{tap0}}$, $\boldsymbol{B}_{\text{tap},s}$, $\boldsymbol{B}_{\text{tap}}$, $y(t)$, $z(t)$, and $u(t)$. The shifting models described by (10)-(14), (16), and (17) are linear constraints that can be solved using MILP.

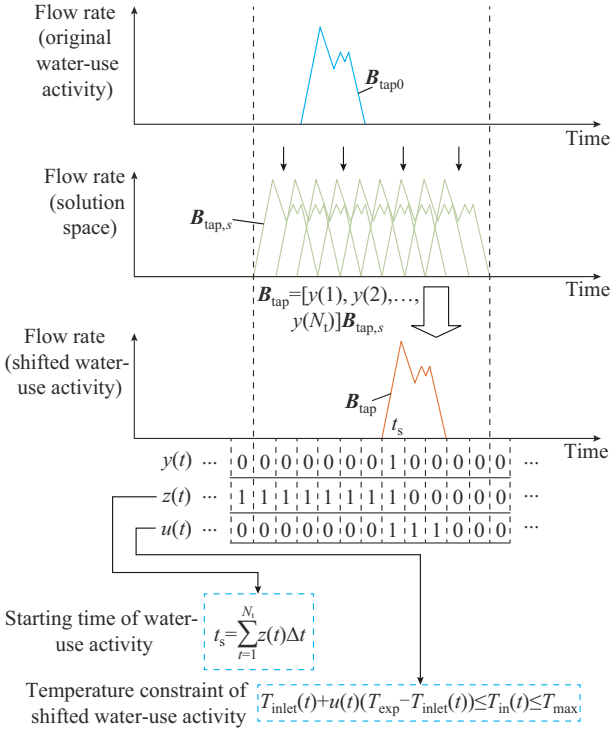

Fig. 5. Shifting model of water-use activity.

IV. Development of EWH Optimization Model

A. Objective Function

The price-based optimization of an individual EWH aims to minimize electricity costs. Considering the monolithically shifted water-use activities, comfort costs should also be considered. The objective function can be formulated as:

$$\min C_{\text{total}}=C_{\text{elec}}+C_{\text{cmft}} \tag{18}$$

where C_{elec} and C_{cmft} are the electricity and comfort costs, respectively.

The electricity cost C_{elec} is the sum of the electricity costs of all periods in the scheduling horizon.

$$C_{\text{elec}}=\sum_{t=1}^{N_{\text{t}}} p_{\text{elec}}(t)P_{\text{e}}(t)\Delta t \tag{19}$$

where $p_{\text{elec}}(t)$ is the electricity price.

The comfort cost C_{cmft} can be represented by the length of the shifted-ahead or delayed water-use time as:

$$C_{\text{cmft}}=p_{\text{cmft}}\left|t_{\text{s}}-t_{\text{s0}}\right| \tag{20}$$

where t_{s0} is the original starting time of the water-use activity; and p_{cmft} is the comfort price (comfort cost per unit shifted time). To be solved by MILP, (20) needs to be further transformed into the following equivalent form:

$$C_{\text{cmft}} = p_{\text{cmft}}(\sigma_+ + \sigma_-) \tag{21}$$

$$t_s = t_{s0} + \sigma_+ - \sigma_- \tag{22}$$

where σ_+ and σ_- are two auxiliary variables that satisfy:

$$\begin{cases} \sigma_+ \geq 0 \\ \sigma_- \geq 0 \end{cases} \tag{23}$$

B. Constraints

1) Thermodynamic Constraint

The thermodynamic constraint is formulated using the discrete thermodynamic models represented by (6) and (9).

2) Shifting Model Constraints

The shifting model constraint is described by (10)-(14), (16), and (17).

3) Water with Shifting Time Limit Constraints

The shifted starting time of the water-use activity t_s should be limited within the range.

$$t_{s,\min} \leq t_s \leq t_{s,\max} \tag{24}$$

where $t_{s,\min}$ and $t_{s,\max}$ are the minimum and maximum allowable limits of t_s, respectively.

4) Electrical Power Limit Constraints

The electrical power $P_e(t)$ should be limited to the nominal power range.

$$0 \leq P_e(t) \leq P_N \tag{25}$$

where P_N is the nominal power of the EWH.

5) Initial Temperature Constraints

The initial temperature constraint defines the initial value of the water temperature.

$$T_{\text{in}}(1) = T_{\text{in1}} \tag{26}$$

where T_{in1} denotes the initial water temperature $T_{\text{in}}(t)$.

C. Summary of Optimization Model

In summary, the optimization model includes the objective functions (18), (19), (21)-(23) and constraints (6), (9), (10)-(14), (16), (17), (24)-(26).

By solving the optimization problem based on MILP, the global optimum of the decision variables $B_{\text{tap}}(t)$ and $P_e(t)$ can be obtained to guide the adjustment of both water-use shifting and electricity use.

V. Testing Examples

A. Experimental Setup

The test examples are based on the Haier LEC6001-CC EWH model. The key parameters of the EWH are listed in Table II. The thermal resistance R, which cannot be directly obtained from the nameplate, is calculated by trial and error. Using the parameters in Table II, (6), and (9), the simulated tank water temperature $T_{\text{in}}(t)$ is calculated and compared with the actual recorded $T_{\text{in}}(t)$, as shown in Fig. 6(a). The manually recorded on/off electrical power status and water-use activities are shown in Fig. 6(b) and (c), respectively. The simulated $T_{\text{in}}(t)$ is very close to the actual recorded $T_{\text{in}}(t)$, indicating that the thermodynamic models of (6) and (9) with the parameters in Table II describe the thermal characteristics of the EWH well.

TABLE II
Key Parameters of EWH

Parameter	Value
c	4200 J/(kg·℃)
ρ	1000 kg/m^3
V_{tank}	0.06 m^3
P_N	2 kW
$T_{\max}$	75 ℃
T_{amb}	12 ℃
T_{inlet}	12 ℃
T_{exp}	40 ℃
R	600 ℃/kW

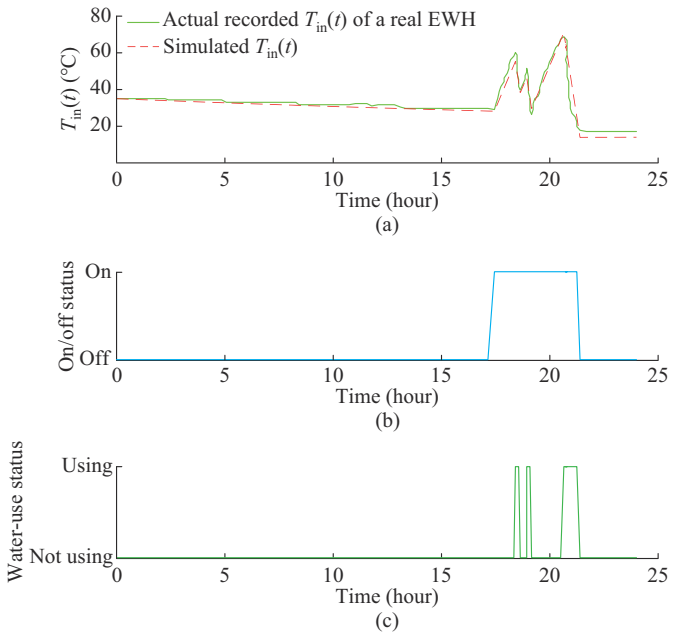

Fig. 6. Simulated tank water temperature $T_{\text{in}}(t)$ versus actual recorded $T_{\text{in}}(t)$. (a) Tank water temperature $T_{\text{in}}(t)$. (b) On/off status of recorded electrical power. (c) Recorded water-use activities.

In addition to the EWH model, the electricity price is an important factor that needs to be considered. In the following examples, the electricity price refers to the time-of-use (TOU) electricity price for residential users in Jiangsu Province. The peak price p_{peak}, which is 0.5583 ¥/kWh, is implemented from 08:00 to 21:00, whereas the valley price p_{valley}, which is 0.3583 ¥/kWh, is implemented during other periods of the day.

Regarding water-use activities, the testing examples are based on the following assumptions.

1) Assuming uniform sampling, error-free signal transmission, and accurate parameters.

2) Assuming that all users are rational and capable of determining the optimal water usage and heating time based on electricity prices and personal comfort demands.

3) Recognizing that different users may have varying time periods for shifting water usage, reflecting the differences in their comfort requirements.

4) Not considering the impact of uncertain factors such as

temporary changes in water demand.

B. Optimization of Single EWH

The proposed method is performed on a single EWH whose key parameters are listed in Table II. To verify the effectiveness of the proposed method, the following three methods are compared.

1) Method 1: no optimization. Water is heated immediately before the water-use activity without considering the TOU price.

2) Method 2: traditional methods. The electrical power of the EWH is optimized by considering the TOU price. However, the shifting of water-use activity is not considered.

3) Method 3: the proposed method. The electrical power of the EWH is optimized by considering both the TOU price and the shifting of the water-use activity.

The original water-use activity is assumed to be between 19:00 and 20:00, representing dish-washing and bathing activities. Note that this may only be one of the typical water-use activities in China, as water-use activities may differ owing to habits, customs, etc.

The optimization results for a single EWH using Methods 1-3 are shown in Fig. 7. From Fig. 7, the following remarks can be observed.

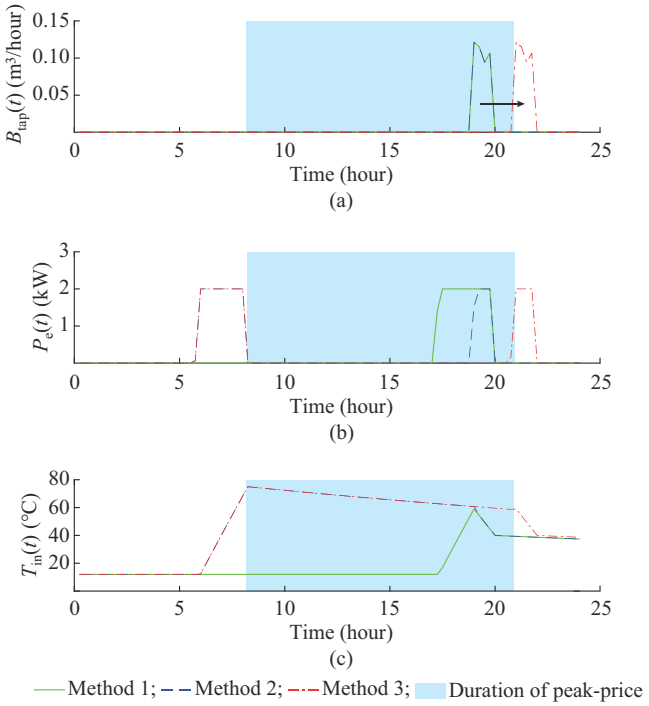

Fig. 7. Optimization results for a single EWH. (a) Flow rate of tap $B_{tap}(t)$. (b) Electrical power $P_e(t)$. (c) Tank water temperature $T_{in}(t)$.

1) Method 1 heats the water tank just before the water-use activity, without considering utilizing the valley electricity price.

2) Method 2 attempts to preheat the EWH during the valley electricity price before 08:00. During the water-use activity, the EWH is heated again to ensure adequate hot water.

3) Method 3 (the proposed method) postpones the water-use activity until 21:00 to utilize the valley electricity price.

Table III lists the energy consumption and electricity costs of the EWH using Methods 1-3. Method 3 (the proposed method) consumes the most electricity energy but has the lowest electricity cost.

TABLE III
ENERGY CONSUMPTION AND ELECTRICITY COSTS OF EWH USING METHODS 1-3

Method	Energy consumption (kWh)	Electricity cost (¥)
Method 1	6.0763	3.3924
Method 2	7.0959	3.0583
Method 3	7.2559	2.8477

C. Optimization of Aggregate EWHs

To illustrate the performance of the proposed method on aggregate EWHs, the parameters of the EWHs are randomized based on Table II, with a relative standard deviation of 0.05. To perform price-based optimization, individual EWHs are optimized, and the aggregate power could be obtained by summing the individual optimization results. The aggregate flow rate and electrical power of the EWHs are denoted by $B_{\text{tap, agg}}(t)$ and $P_{\text{e, agg}}(t)$, respectively. $B_{\text{tap, agg}}(t)$ and $P_{\text{e, agg}}(t)$ can be formulated as :

$$B_{\text{tap, agg}}(t) = \sum_{i=1}^{N_{\text{EWHs}}} B_{\text{tap},i}(t) \tag{27}$$

$$P_{\text{e, agg}}(t) = \sum_{i=1}^{N_{\text{EWHs}}} P_{\text{e},i}(t) \tag{28}$$

where $B_{\text{tap},i}(t)$ and $P_{\text{e},i}(t)$ are the flow rate and electrical power of the i^{th} EWH, respectively; and N_{EWHs} is the total number of EWHs.

Considering 100 EWHs in the price-based DR, the optimization results of the aggregate EWHs are shown in Fig. 8, and the optimization results of five randomly selected EWHs are shown in Fig. 9.

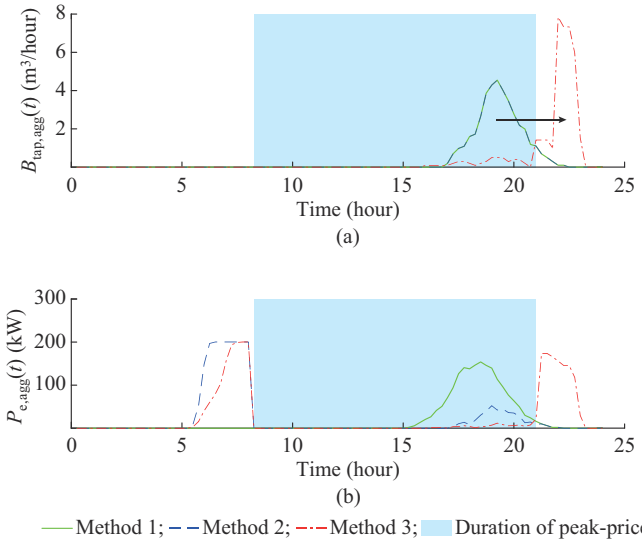

Fig. 8. Optimization results of aggregate EWHs. (a) Aggregate flow rate $B_{\text{tap, agg}}(t)$. (b) Aggregate electrical power $P_{\text{e, agg}}(t)$.

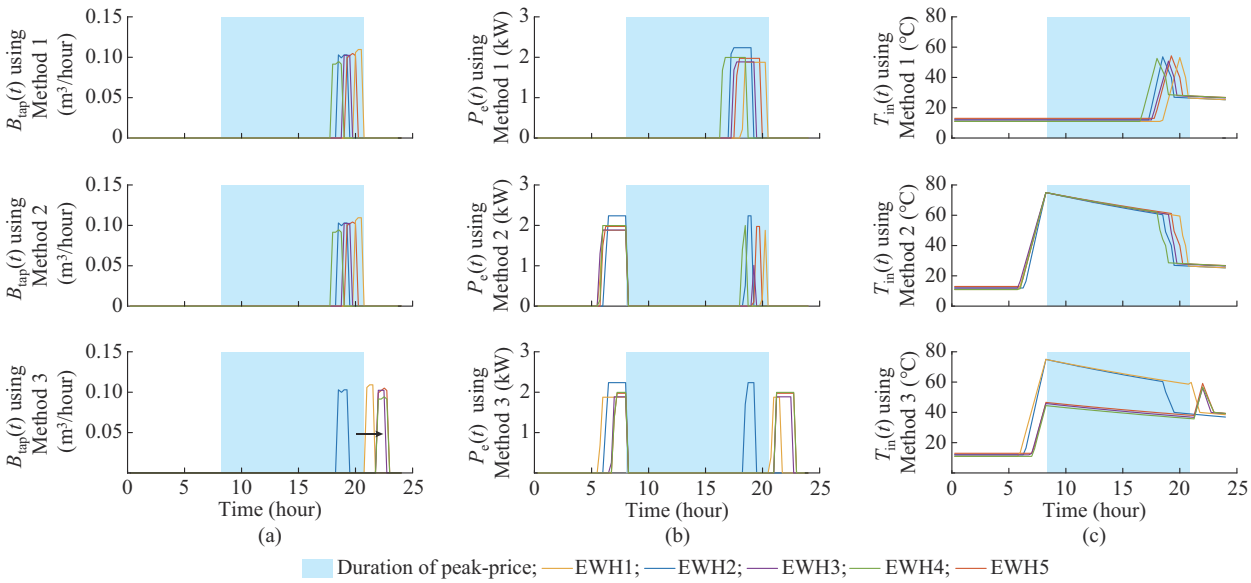

Fig. 9. Optimization results for five randomly selected EWHs. (a) Flow rate of tap $B_{tap}(t)$. (b) Electrical power $P_e(t)$. (c) Tank water temperature $T_{in}(t)$.

To demonstrate the peak-shaving performance of different methods, Fig. 10 presents the curves of the total electrical load by adding the aggregate load of the EWHs to the actual electrical load data. From Figs. 8-10, the following observations can be obtained.

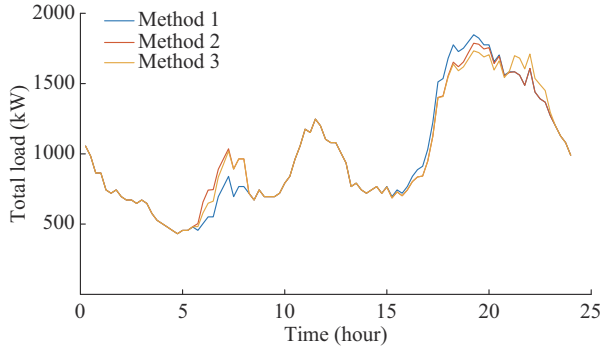

Fig. 10. Peak-shaving performance using different methods.

1) The optimization results of the aggregate EWHs shown in Fig. 8 are similar to those of a single EWH (as shown in Fig. 7). Method 3 postpones the aggregate water-use activities until after 21: 00 to utilize the lower valley electricity price.

2) Figure 9 shows that different users perform similarly under the uniform peak-valley TOU price. In Method 3, the tank water is preheated, and water-use activities are postponed by most users.

3) Figure 10 shows that both Methods 2 and 3 can shift the peak load to off-peak hours. Compared with Method 2, Method 3 shifts the peak load more, and the maximum load is lower, which is therefore more beneficial to the stability of the power system.

Table IV lists the aggregate energy consumption and aggregate electricity cost of the EWHs using Methods 1-3. Method 3 results in the lowest electricity cost, which is in accordance with Table III.

TABLE IV
AGGREGATE ENERGY CONSUMPTION AND AGGREGATE ELECTRICITY COST OF EWHS USING METHODS 1-3

Method	Aggregate energy consumption (kWh)	Aggregate electricity cost (¥)
Method 1	526.7589	290.9868
Method 2	632.3078	260.1719
Method 3	609.6932	227.4769

D. Influence of Electricity Price on Optimization Results

The electricity price, which can be adjusted according to the requirements of power system, is a key factor that affects the optimization results of EWHs. To investigate the influence of the electricity price on the optimization results, the following two indicators are considered for the analysis.

1) Starting time of the valley price t_{vs}: the moment when the TOU electricity price changes from peak price p_{peak} to valley price p_{valley}. To ensure that the durations of the peak and valley prices are consistent, the starting time of the peak price is adjusted by t_{vs}.

2) Peak-valley ratio K: it is defined as $K=p_{peak}/p_{valley}$, indicating the peak-valley difference in the TOU electricity price. To ensure that the average price is consistent, p_{peak} and p_{valley} are calculated for a given K.

The definitions of t_{vs} and K are shown in Fig. 11.

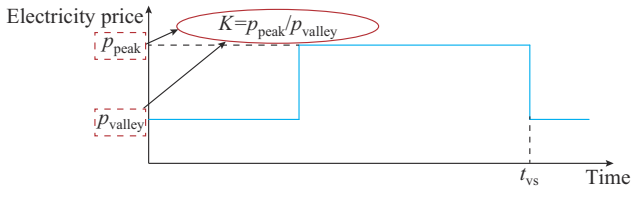

Fig. 11. Definitions of t_{vs} and K.

The optimization results for the t_{vs} values of hour 19, hour 20, hour 21, and hour 22 are shown in Fig. 12, and the con-

tour map of the influence of t_{vs} on the optimization results is shown in Fig. 13. The optimization tends to postpone the water-use activities until t_{vs} to utilize the valley price. However, if t_{vs} is too late (e. g., $t_{vs}=22$ hours), a large number of EWHs will not postpone the water-use activities. These EWHs consume more electricity early in the morning to utilize the valley price.

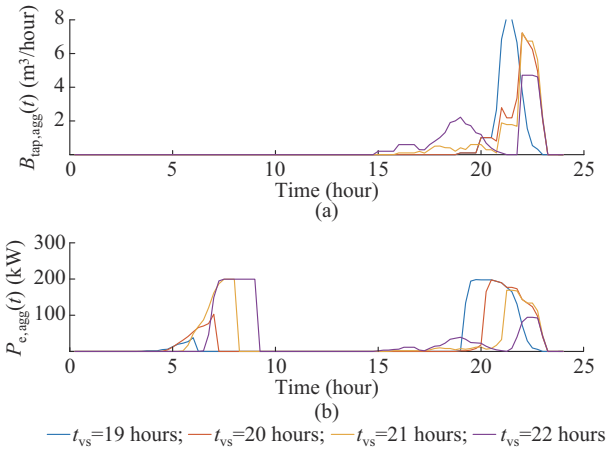

Fig. 12. Optimization results for different values of t_{vs}. (a) Aggregate flow-rate $B_{tap,agg}(t)$. (b) Aggregate electrical power $P_{e,agg}(t)$.

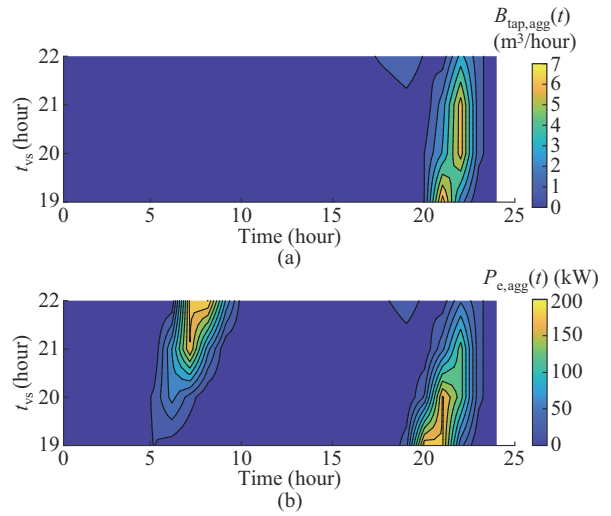

Fig. 13. Influence of t_{vs} on optimization results. (a) Influence of t_{vs} on optimized $B_{tap,agg}(t)$. (b) Influence of t_{vs} on optimized $P_{e,agg}(t)$.

The optimization results for different values of K (1, 1.3, 1.6, and 1.9) are shown in Fig. 14, and the contour map of the influence of K on the optimization results is shown in Fig. 15. A larger value of K tends to postpone more water-use activities to utilize the valley price and leads to more electricity consumption early in the morning and late at night to utilize the valley price.

E. Sensitivity Analysis of Comfort Price

The comfort price p_{cmft} reflects the users' willingness to shift water-use activities and has a significant impact on the optimization results of EWHs. In this subsection, a sensitivity analysis is conducted on the comfort price p_{cmft} to determine the approximate range of p_{cmft} required for noticeable EWH load-shifting.

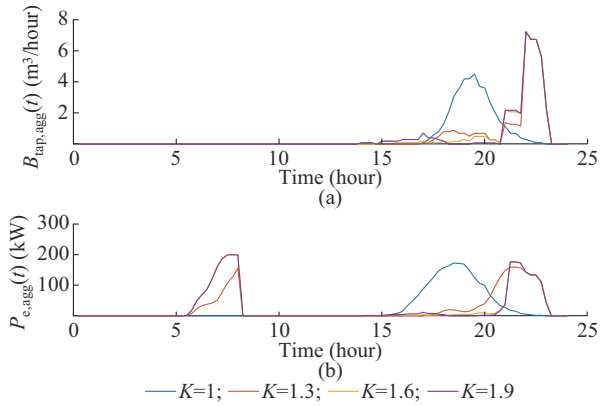

Fig. 14. Optimization results for different values of K. (a) Aggregate flow rate $B_{tap,agg}(t)$. (b) Aggregate electrical power $P_{e,agg}(t)$.

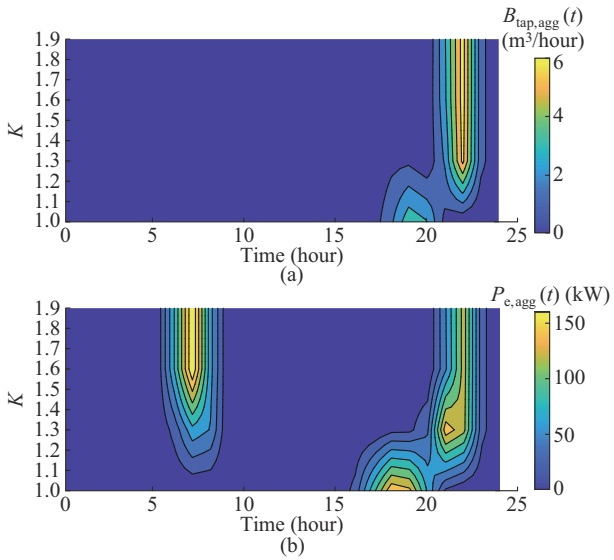

Fig. 15. Influence of K on optimization results. (a) Influence of K on optimized $B_{tap,agg}(t)$. (b) Influence of K on optimized $P_{e,agg}(t)$.

This case study considers 100 EWHs. Assuming that the comfort price p_{cmft} varies from 0 to 0.45 ¥/hour, the influence of p_{cmft} on the optimization results is investigated. The aggregate flow rates and electrical power of the 100 EWHs are shown in Fig. 16(a) and (b), respectively.

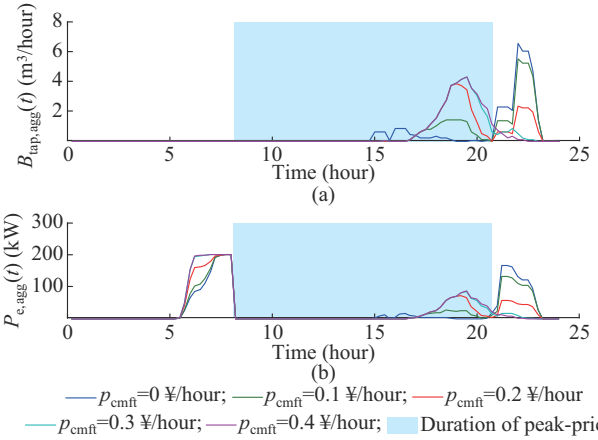

Fig. 16. Optimization results for different values of p_{cmft}. (a) Aggregate flow rate $B_{tap,agg}(t)$. (b) Aggregate electrical power $P_{e,agg}(t)$.

The optimization results for five randomly selected EWHs with different values of p_{cmft} out of the 100 EWHs are shown in Fig. 17. The statistical results of the impact of p_{cmft} on water-use activities and the corresponding contour maps are shown in Fig. 18.

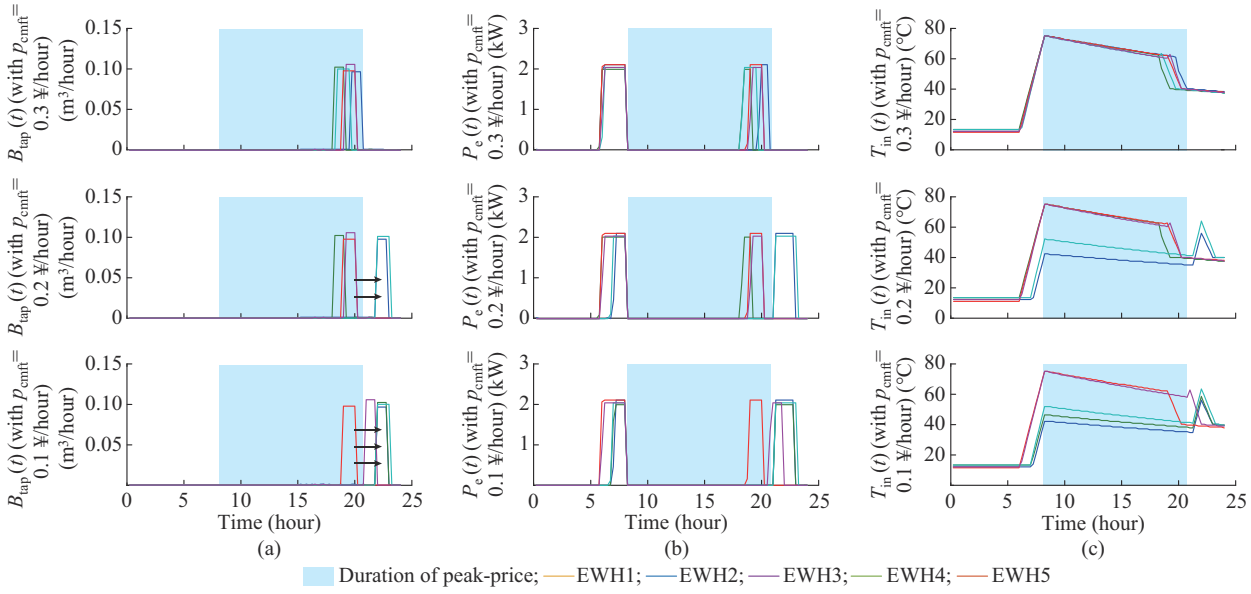

Fig. 17. Optimization results for five randomly selected EWHs with different values of p_{cmft}. (a) Flow rate of tap $B_{\text{tap}}(t)$. (b) Electrical power $P_{\text{e}}(t)$. (c) Tank water temperature $T_{\text{in}}(t)$.

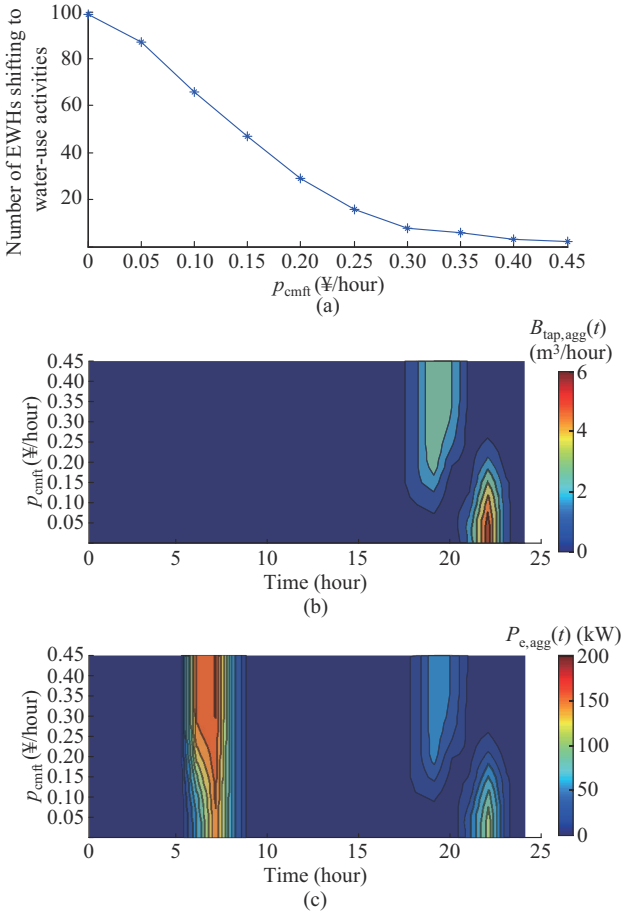

Fig. 18. Statistical results of impact of p_{cmft} on water-use activities and corresponding contour maps of $B_{\text{tap,agg}}(t)$ and $P_{\text{e,agg}}(t)$. (a) Influence of p_{cmft} on number of EWHs shifting to water-use activities. (b) Influence of p_{cmft} on optimized $B_{\text{tap,agg}}(t)$. (c) Influence of p_{cmft} on optimized $P_{\text{e,agg}}(t)$.

From Figs. 16-18, the following remarks can be obtained.

1) The comfort price p_{cmft} had a significant impact on the shifting of water-use activities, which is reflected by the flow rate of the tap $B_{\text{tap,agg}}(t)$ (Figs. 16(a) and 18(b)), and the number of EWHs shifting the water-use activities (Fig. 18(a)). A smaller value of p_{cmft} leads to more EWHs shifting water-use activities. The aggregate tap flow rate $B_{\text{tap,agg}}(t)$ further determines the aggregate electrical power $P_{\text{e,agg}}(t)$ (Figs. 16(b) and 18(c)).

2) For individual EWHs, when p_{cmft} is smaller, more EWHs shift the water-use activities to hour 21, or even later, and the majority of these EWHs take advantage of lower off-peak electricity prices after hour 21. There is a significant heating process in the tank water temperature $T_{\text{in}}(t)$ after hour 21 (Fig. 17).

3) As p_{cmft} varies from 0 to 0.45 ¥/hour, the percentage of EWHs involved in the shifting of water-use activities decreases from approximately 100% to close to 0% (Fig. 18(a)). When p_{cmft} exceeds 0.3 ¥/hour, very few EWHs are involved in the shifting of water-use activities. However, when p_{cmft} is below 0.2 ¥/hour, there is a noticeable shift in the water-use activities among the EWHs, and when p_{cmft} is below 0.1 ¥/hour, the shift in water-use activities becomes highly significant.

VI. Conclusion

This paper proposes a scheduling method for EWHs that considers the shifting potential of water-use activities, by which the water-use activities could be monolithically shifted in the scheduling horizon. The key findings of this paper are summarized as follows.

1) The proposed method can shift water-use activities, and

therefore increase the load-shifting potential of EWHs.

2) The proposed method leads to higher energy consumption but lower electricity costs under the TOU peak-valley price.

3) The starting time of the valley price and the peak-valley ratio are the two key indices that affect the water-use shifting potential and load-shifting potential of EWHs.

Future studies should investigate the frequency control capacity of EWHs under water-use activities and develop a corresponding scheduling and control model for the power system.

REFERENCES

[1] Y. Bao, P. Chen, M. Hu *et al.*, "Control parameter optimization of thermostatically controlled loads using a modified state-queuing model," *CSEE Journal of Power and Energy Systems*, vol. 6, no. 2, pp. 394-401, Jun. 2020.

[2] Y. Bao, X. Zhou, T. Ji *et al.*, "Power fluctuation damping of thermostatically controlled loads based on state estimation," *CSEE Journal of Power and Energy Systems*, vol. 6, no. 4, pp. 834-840, Dec. 2020.

[3] Z. Zheng, J. Pan, G. Huang *et al.*, "A bottom-up intra-hour proactive scheduling of thermal appliances for household peak avoiding based on model predictive control," *Applied Energy*, vol. 323, p. 119591, Oct. 2022.

[4] A. Maiorino, M. G. Del Duca, A. Mota-Babiloni *et al.*, "Achieving a running cost saving with a cabinet refrigerator incorporating a phase change material by the scheduling optimisation of its cyclic operations," *International Journal of Refrigeration*, vol. 117, pp. 237-246, Sept. 2020.

[5] P. J. C. Nel, M. J. Booysen, and B. Van Der Merwe, "Horizontal electric water heaters with scheduling," *IEEE Transactions on Smart Grid*, vol. 9, no. 1, pp. 48-56, Jan. 2018.

[6] H. Gong, T. Rooney, O. M. Akeyo *et al.*, "Equivalent electric and heat-pump water heater models for aggregated community-level demand response virtual power plant controls," *IEEE Access*, vol. 9, pp. 141233-141244, Oct. 2021.

[7] S. Xiang, L. Chang, B. Cao *et al.*, "A novel domestic electric water heater control method," *IEEE Transactions on Smart Grid*, vol. 11, no. 4, pp. 3246-3256, Jul. 2020.

[8] S. A. Pourmousavi, S. N. Patrick, and M. H. Nehrir, "Real-time demand response through aggregate electric water heaters for load shifting and balancing wind generation," *IEEE Transactions on Smart Grid*, vol. 5, no. 2, pp. 769-778, Jul. 2014.

[9] W. Mendieta and C. A. Canizares, "Primary frequency control in isolated microgrids using thermostatically controllable loads," *IEEE Transactions on Smart Grid*, vol. 12, no. 1, pp. 93-105, Jan. 2021.

[10] J. Xu, H. Mahmood, H. Xiao *et al.*, "Electric water heaters management via reinforcement learning with time-delay in isolated microgrids," *IEEE Access*, vol. 9, pp. 132569-132579, Sept. 2021.

[11] T. Peirelinck, C. Hermans, F. Spiessens *et al.*, "Domain randomization for demand response of an electric water heater," *IEEE Transactions on Smart Grid*, vol. 12, no. 2, pp. 1370-1379, Jul. 2021.

[12] F. Ruelens, B. J. Claessens, S. Quaiyum *et al.*, "Reinforcement learning applied to an electric water heater: from theory to practice," *IEEE Transactions on Smart Grid*, vol. 9, no. 4, pp. 3792-3800, Jul. 2018.

[13] H. Kazmi, F. Mehmood, S. Lodeweyckx *et al.*, "Gigawatt-hour scale savings on a budget of zero: deep reinforcement learning based optimal control of hot water systems," *Energy*, vol. 144, pp. 159-168, Feb. 2018.

[14] M. Zu, "Electric water heaters using dynamic programming and *K*-means clustering," *IEEE Transactions on Sustainable Energy*, vol. 11, no. 1, pp. 524-533, Jan. 2020.

[15] S. Pang, Z. Zheng, X. Xiao *et al.*, "Collaborative power tracking method of diversified thermal loads for optimal demand response: an MILP-based decomposition algorithm," *Applied Energy*, vol. 327, p. 120006, Oct. 2022.

[16] C. H. Antunes, M. J. Alves, and I. Soares, "A comprehensive and modular set of appliance operation MILP models for demand response optimization," *Applied Energy*, vol. 320, p. 119142, Jun. 2022.

[17] F. Najafi and M. Fripp, "Stochastic optimization of comfort-centered model of electrical water heater using mixed integer linear programming," *Sustainable Energy Technologies and Assessments*, vol. 42, p. 100834, Mar. 2020.

[18] M. Wu, Y. Bao, J. Zhang *et al.*, "Multi-objective optimization for electric water heater using mixed integer linear programming," *Journal of Modern Power Systems and Clean Energy*, vol. 7, no. 5, pp. 1256-1266, Sept. 2019.

[19] N. Cammardella, A. Bušić, and S. Meyn, "Simultaneous allocation and control of distributed energy resources via Kullback-Leibler-Quadratic optimal control," in *Proceedings of 2020 American Control Conference (ACC)*, Denver, USA, Jul. 2020, pp. 514-520.

Yuqing Bao received the Ph. D. degree from Southeast University (SEU), Nanjing, China, in 2016, and works as a Faculty Member at Nanjing Normal University, Nanjing, China, since December 2015. His current research interests include power system operation and scheduling, power demand side management, and frequency control of power systems.

Zhonghui Zuo received the B. S. degree from Nanjing Normal University, Nanjing, China, in 2021. She is currently pursuing the M. S. degree with Nanjing Normal University. Her research interests include power system operation and scheduling.

Xuehua Wu received the B.S. degree in electrical engineering and the M.S. degree in power system and its automation from Nanjing University of Aeronautics and Astronautics (NUAA), Nanjing, China, in 2009 and 2012, respectively. She received the Ph.D. degree from Southeast University, Nanjing, China, in 2021, and works as a Faculty Member at Nanjing Vocational University of Industry Technology, Nanjing, China, since October 2021. Her current research interests include intelligence algorithms and their applications.